JOURNAL OF THE ROYAL SOCIETY Interface

J. R. Soc. Interface (2008) **5**, 1309–1316
doi:10.1098/rsif.2008.0017
Published online 8 April 2008

Anterior-to-posterior wave of buccal expansion in suction feeding fishes is critical for optimizing fluid flow velocity profile

Kristin L. Bishop*, Peter C. Wainwright and Roi Holzman

Section of Evolution and Ecology, University of California, Davis, CA 95616, USA

In fishes that employ suction feeding, coordinating the timing of peak flow velocity with mouth opening is likely to be an important feature of prey capture success because this will allow the highest forces to be exerted on prey items when the jaws are fully extended and the flow field is at its largest. Although it has long been known that kinematics of buccal expansion in feeding fishes are characterized by an anterior-to-posterior wave of expansion, this pattern has not been incorporated in most previous computational models of suction feeding. As a consequence, these models have failed to correctly predict the timing of peak flow velocity, which according to the currently available empirical data should occur around the time of peak gape. In this study, we use a simple fluid dynamic model to demonstrate that the inclusion of an anterior-to-posterior wave of buccal expansion can correctly reproduce the empirically determined flow velocity profile, although only under very constrained conditions, whereas models that do not allow this wave of expansion inevitably predict peak velocity earlier in the strike, when the gape is less than half of its maximum. The conditions that are required to produce a realistic velocity profile are as follows: (i) a relatively long time lag between mouth opening and expansion of the more posterior parts of the mouth, (ii) a short anterior portion of the mouth relative to more posterior sections, and (iii) a pattern of movement that begins slowly and then rapidly accelerates. Greater maximum velocities were generated in simulations without the anterior-to-posterior wave of expansion, suggesting a trade-off between maximizing fluid speed and coordination of peak fluid speed with peak gape.

Keywords: suction feeding; fluid dynamics; biomechanics

1. INTRODUCTION

Many fishes capture prey using a suction mechanism in which the oral cavity is rapidly expanded to create a flow of water into the mouth. The prey item becomes entrained in this flow and is drawn into the mouth. The flow can reach a high velocity, but lasts only a few milliseconds and extends only about one mouth diameter in front of the fish (Day *et al.* 2005). As a result, the temporal pattern of the flow created by the fish is critically important to prey capture success (Holzman *et al.* 2007). For example, if the flow draws the prey towards the mouth of the fish at a time when the gape is not wide enough to accommodate it, the prey may have an opportunity to escape. Many fishes enhance their strikes by quickly protruding their jaws, allowing a stealthier attack. This action will be most effective if the timing of the production of the greatest fluid forces on the prey item is coordinated with maximum jaw protrusion. A consideration of the fluid dynamics underlying the coordination of fluid flow with movements of the mouth can provide substantial insight into this important interaction.

*Author for correspondence (kvwbishop@ucdavis.edu).

It has long been noted that the expansion of the buccal cavity occurs in an anterior-to-posterior wave (Lauder 1980*a*; Sanford & Wainwright 2002; Van Wassenbergh *et al.* 2004; Gibb & Ferry-Graham 2005), such that the mouth opens first, followed by depression of the hyoid, abduction of the suspensoria and finally abduction of the opercula. This anterior-to-posterior wave of expansion appears to be ubiquitous among suction feeding fishes, having apparently been found in every species studied to date including a diverse array of teleosts (Lauder 1980*b*; Sanford & Wainwright 2002; Van Wassenbergh *et al.* 2004; Gibb & Ferry-Graham 2005), non-teleost actinopterygian fishes (Lauder 1980*a*; Carroll & Wainwright 2003) and chondrichthians (Ferry-Graham 1997; Wilga & Motta 1998*a*,*b*; Motta *et al.* 2002), as well as aquatically feeding tetrapods such as salamanders (Lauder & Shaffer 1985; Reilly 1995) and turtles (Summers *et al.* 1998). Although some authors have speculated that this pattern probably promotes unidirectional flow during the strike (Ferry-Graham & Lauder 2001; Gibb & Ferry-Graham 2005), no serious consideration has been given to why this should be so widespread a feature of suction feeding.

Received 16 January 2008
Accepted 20 March 2008

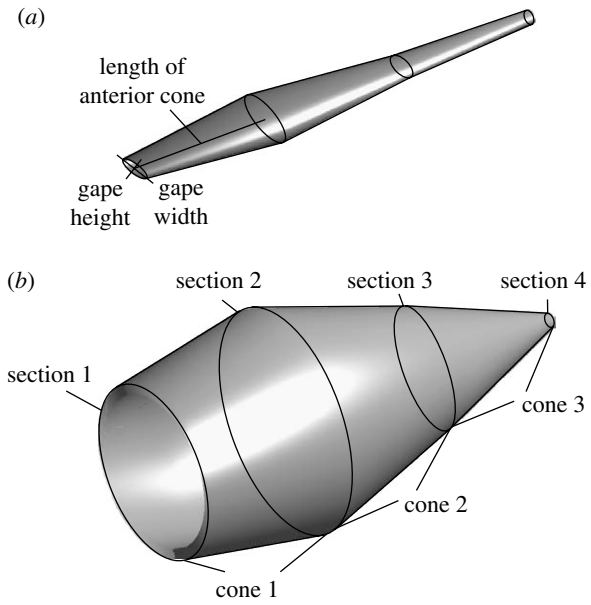

Figure 1. Buccal cavity geometry consisting of three interconnected, truncated, elliptical cones in (*a*) unexpanded and (*b*) fully expanded configurations. In this example, the length of the buccal cavity is roughly equally distributed between the three cones. In the computational model, the buccal cavity length can be distributed in any way between the three cones.

In past efforts to model fluid flow during suction feeding, the expanding mouths of fishes have been represented geometrically as either an expanding cylinder (Drost *et al.* 1988), a truncated cone (Muller *et al.* 1982; van Leeuwen & Muller 1983, 1984), a series of elliptical cylinders (Van Wassenbergh *et al.* 2006*b*) or a series of three interconnected expanding truncated cones (Van Wassenbergh *et al.* 2006*a*; figure 1). The single-cone representation of the fish mouth can be modelled with no wave of expansion by making the entire buccal cavity expand simultaneously, or it is possible to crudely model an expansion wave by building in a time delay between expansion of the two ends of the cone. With a model using multiple interconnected cone geometry, it is possible to use time delays for each end of each cone to create a true wave of expansion.

Previous models using a single-cone geometry have predicted the time course of flow velocity during a feeding strike poorly. Recent experiments using particle image velocimetry (PIV) to measure the flow speed in front of the mouths of feeding bluegill sunfish and largemouth bass have found that the maximum flow velocity occurs either just before or concurrently with maximum gape (Ferry-Graham *et al.* 2003; Day *et al.* 2005; Higham *et al.* 2006). While similar measurements have yet to be made in other taxa, this finding is not consistent with earlier model results based on an expanding cone, which predicted that maximum flow velocity occurs much earlier in the strike (Muller *et al.* 1982; van Leeuwen & Muller 1983).

These earlier models have greatly improved our understanding of suction feeding and have made accurate predictions about important features of suction feeding. The single-cone model of van Leeuwen & Muller (1984) predicted the largest prey velocities to occur at

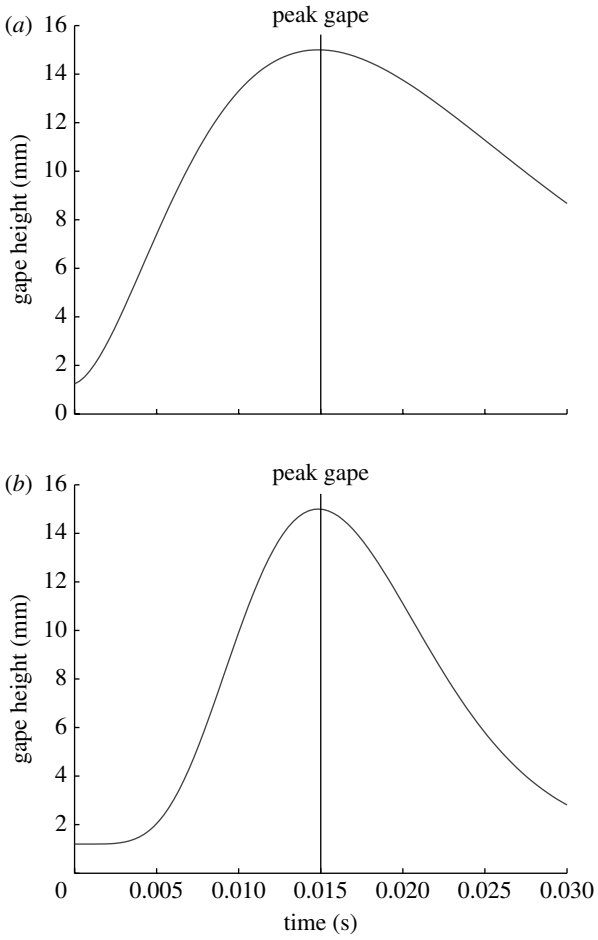

Figure 2. Sample kinematic profiles for gape height using differing values of α. (*a*) $\alpha=2$, the velocity is relatively constant throughout mouth opening. (*b*) $\alpha=7$, mouth opening begins very slowly, then accelerates quickly to reach a high velocity and then decelerates again as peak gape is reached.

the time the prey crosses the plane of the mouth opening, which corresponded to the time of peak gape. This prediction was consistent with kinematic data from five species of fishes (van Leeuwen & Muller 1984). However, this study did not directly address the time course of fluid speed at the mouth opening. A more recent model represented the geometry of the buccal cavity as a series of elliptical cylinders and used video data for feeding catfishes to determine the dimensions of the cylinders throughout the simulated strike (Van Wassenbergh *et al.* 2006*b*). This model predicted maximum flow velocities near the time of peak gape, as was found empirically for the bluegill sunfish and largemouth bass. However, this approach requires highly detailed kinematic information that is labour intensive to obtain.

A model using a simplified geometry that reproduces important features of suction feeding in living fishes will allow predictions to be made about the consequences of changes in morphology and kinematics to suction feeding performance, but previous simplified models have failed to accurately predict the time course of fluid flow velocity relative to the gape cycle. This discrepancy has raised questions about the accuracy of these models (Day *et al.* 2005), but an adequate explanation has yet to be given for it.

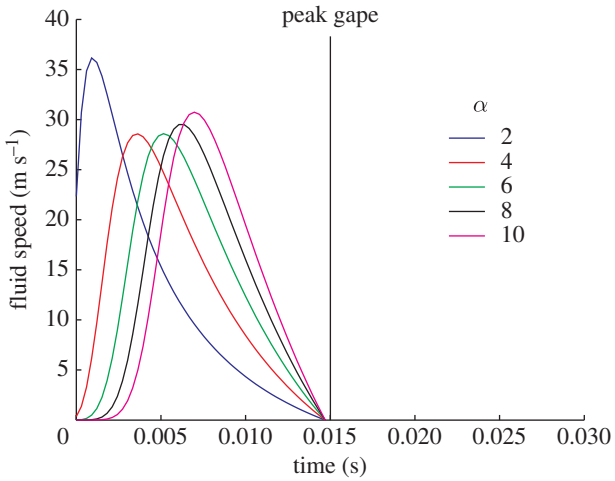

Figure 3. Fluid velocity at the mouth opening for a single elliptical cone geometry with no delay in the onset of the expansion of the posterior end of the cone at a range of α values. At all values of α, fluid velocity reaches zero by the time of peak gape. Model parameters: anterior starting height, 1.2 mm; anterior starting width, 3.2 mm; anterior maximum height, 15 mm; anterior maximum width, 15 mm; posterior starting height, 3.6 mm; posterior starting width, 6 mm; posterior maximum height, 15.8 mm; posterior maximum width, 19.8 mm; mouth length, 40 mm; and total strike time, 30 ms.

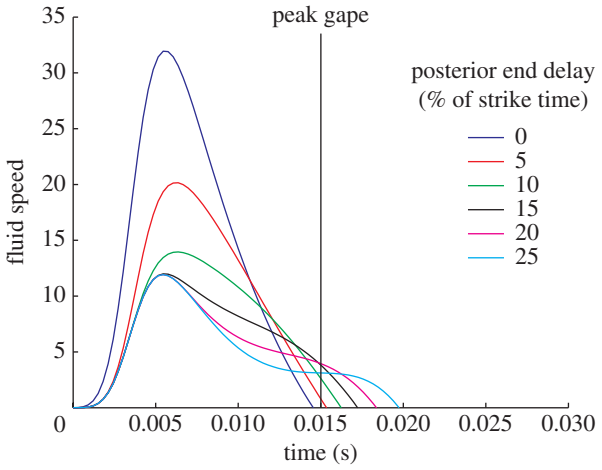

Figure 4. Flow velocity profiles for single round cone geometries with onset delays for the posterior end ranging from 0 to 25% of the strike time at $\alpha=7$. Even with delayed posterior expansion, the velocity peak never occurred later than 20% of total strike time. The magnitude of the peak velocity decreases as the volume expansion is distributed through a larger portion of the strike by the posterior delays. Model parameters: anterior starting diameter, 1.2 mm; anterior maximum diameter, 15 mm; posterior starting diameter, 3.6 mm; posterior maximum diameter, 15.8 mm; mouth length, 40 mm; $\alpha=7$; total strike time, 30 ms.

The purpose of this paper is to use a fluid dynamic model with a relatively simple geometric representation of the buccal cavity to attempt to reconcile the empirically determined velocity profile of a feeding fish with that predicted computationally by incorporating an anterior-to-posterior wave of expansion of the buccal cavity. We are specifically interested in identifying the features of buccal expansion patterns that result in peak suction flow speed occurring near the time of maximum mouth opening. We base the kinematic profiles of the oral expansion on those of a 19 cm bluegill sunfish (*Lepomis macrochirus*) to allow direct comparison of the model output with prior empirical results. We compare model results based on a single expanding truncated cone and three interconnected truncated cones with empirical fluid velocity profiles of the feeding bluegill sunfish to examine the effect of incorporating an anterior-to-posterior wave of oral expansion.

2. METHODS

To test the effect of an anterior-to-posterior wave of oral expansion on fluid velocity at the mouth, we developed a computational model based on the law of continuity. According to the law of continuity, the fluid velocity at the mouth opening (v) at any given time during a feeding strike is equal to the change in volume (V) of the buccal cavity since the previous time step divided by the area of the mouth opening (A):

$$v(t) = \frac{\mathrm{d}V/\mathrm{d}t}{A(t)}. \tag{2.1}$$

Thus, fluid velocity is maximized when the mouth opening is small and/or when the rate of change in volume is large.

For our simulations, the total strike time of 30 ms was divided into 100 evenly spaced time steps, with the onset of the mouth opening occurring at time zero and the maximum gape set at 15 ms for all tests. The change in buccal cavity volume was defined by changes in the dimensions of the circles or ellipses at each end of the cone (each end of each cone for the multiple cone model). Following Muller *et al.* (1982), the kinematic profiles with respect to time were calculated for each time step as

$$h(t) = h_0 + (h_{\max} - h_0) \times \left[\frac{(t - t_{\mathrm{lag}})}{(t_{h\,\max} - t_{\mathrm{lag}})} \exp\left\{1 - \frac{(t - t_{\mathrm{lag}})}{(t_{h\,\max} - t_{\mathrm{lag}})}\right\}\right]^{\alpha}, \tag{2.2}$$

where $h(t)$ is the kinematic parameter at time t; h_0 is its initial value; $h_{\max}$ is its maximum value; t_{lag} is the time lag for that section relative to the start of mouth opening; $t_{h\,\max}$ is the time at which the parameter reaches its maximum value; and α is the expansion coefficient of the profile. The expansion coefficient determines the velocity profile for the movement, such that at low values of α the movement occurs steadily with a relatively constant velocity throughout (figure 2*a*), whereas at higher α values the movement begins slowly and rapidly accelerates through the middle of the movement and decelerates again near the end of the movement (figure 2*b*). All calculations were performed using MATLAB (The Mathworks, Natick, MA) on a Macintosh PowerBook G4.

The single-cone geometry was tested for both circular and elliptical cross sections. Simulations were run with two conditions: simultaneous expansion of the anterior and posterior ends of the cone, and with

varying time delays for the expansion of the posterior end of the cone relative to the anterior end. The model was tested at α values of 1–10, which just exceeds the range of 2–9 observed in 15 species of centrarchid fishes (R. Holzman 2007, unpublished data). The three-cone model used elliptical cross sections (Drost & van den Boogaart 1986) and allowed the starting and stopping time of the expansion of each end of each cone to be determined independently, but α was held constant for all sections within a simulated strike. The dimensions of the posterior end of each cone were equal to those of the anterior end of the cone behind it at all times.

The three cones are intended to very roughly represent three areas of the buccal cavity which are capable of moving largely independently: (i) the region from the mouth opening to the anterior hyoid; (ii) the region spanning the anterior-to-posterior length of the hyoid; and (iii) the region posterior to the hyoid extending to the opening of the oesophagus. The posterior end of cone 3 is taken to be the posterior limit of the region of the buccal cavity that is capable of expansion; therefore that ellipse does not expand in the simulations and is relatively small. This approximation is a potential source of error, as there is some uncertainty about the role of the opercular cavities during buccal expansion. If water is able to move freely between the buccal and opercular cavities, it is possible that, although the oesophagus itself does not expand, the posterior end of the chamber expands as a result of opercular abduction, forming something resembling a back wall with a small oesophageal opening in it. Whether water flows freely between these two chambers remains an unresolved issue (Lauder 1983). However, we expect this approximation to have a minimal effect on the results. Although adding another expanding section would alter the magnitude of the maximum fluid velocities, it would allow a more refined anterior-to-posterior wave of expansion; therefore assuming a non-expanding posterior section is conservative with respect to the goal of this study. In addition, Lauder (1980*b*) found that in the bluegill sunfish the abduction of the operculum begins very shortly before peak gape; so the effect of this expansion on the flow profile up to peak gape is expected to be minimal.

The dimensions of the expanded buccal cavity were taken from casts of the fully expanded buccal cavity of bluegill sunfish of a similar size and with similar maximum gape height to the one from which the empirical velocity data were taken. These dimensions were held constant for all of the simulations based on a three-cone geometry. The starting and ending heights of the mouth and the time to peak gape were based on observed gape kinematics of a 190 mm (SL) bluegill sunfish feeding on shrimp, recorded at 500 fps (as in Day *et al.* 2005) with a known fluid velocity profile, and were the same for all models. The maximum dimensions for the posterior end of the single cone were equal to the maximum dimensions of the largest section in the three-cone model. The total length of the buccal cavity for all geometries was 50 mm, but for the three-cone model, the length could be allocated in any way between the three cones.

Morphology and timing variables were manipulated to find combinations that adequately reproduced experimental results for the bluegill sunfish. To explore this parameter space, we ran 598 230 simulations with every combination of α (range 1–10), onset delay of section 2 (range 0–50% of strike), onset delay of section 3 (range 0–50% of strike) and length of cone 1 (range 2–46 mm). Eliminating all simulations in which the onset delay of section 2 was greater than that of section 3 left 304 980 simulations. Of these, simulations were selected that had only a single velocity peak that occurred between 90 and 110 per cent of the time to peak gape, which is the range found using PIV data (Day *et al.* 2005).

It should be noted that none of these models incorporates the opening of the opercular valve, which occurs sometime after peak gape (Lauder 1985). This posterior opening maintains unidirectional flow as the mouth cavity compresses. Without this opening, any decrease in the total volume of the mouth cavity would cause water to flow back out of the mouth (negative velocity in this case). This phenomenon only affects the model after peak gape has occurred and does not alter the timing of peak velocity relative to peak gape. Velocity and volume profiles are shown beyond this point to demonstrate the shape of the theoretical profiles; however, it should be borne in mind that the velocity profiles are not realistic after the time of opercular opening.

3. RESULTS

The single-cone geometry with no time delay produced a velocity profile with zero fluid speed at the time of peak gape at all values of α (figure 3) and for both circular and elliptical cross sections. The time of peak fluid velocity increased with increasing α, with the latest velocity peak occurring at 48 per cent of the time to peak gape at $\alpha = 10$. When the entire buccal cavity expands synchronously, the greatest rate of volume increase occurs when the velocity of the movement is the highest: approximately halfway between the beginning of mouth opening and maximum gape (figure 2). Because the area of the mouth opening is the smallest near the beginning of the strike, the predicted velocity peak is shifted to an even earlier time in this model. At maximum gape, the area of the mouth opening is (by definition) at a maximum and, because the entire buccal cavity expands synchronously, the rate of increase in buccal volume approaches zero as gape approaches its maximum, so flow velocity at the mouth rapidly decreases to zero at maximum gape (figure 3).

The single expanding cone model was tested at posterior end time lags ranging from 0 to 50% of the total strike duration (figure 4). For clarity, only delays up to 25 per cent are shown. At higher delays, there is one velocity peak early in the strike at approximately 35 per cent of the time to peak gape, and a second peak well after peak gape. In all of the simulations with two peaks, there is a local minimum between them, which occurs at the time of peak gape. These simulations yielded velocity profiles with peak velocities at times ranging from 34 to 40% of the time to peak gape, with the latest peak occurring with a time lag of 2.5 per cent

of time to peak gape. Regardless of the time lag used in this model, the expansion of the mouth drives an increase in the volume throughout the oral cavity during the early part of the strike. Because velocity is proportional to the volume change in the buccal cavity and inversely proportional to the area of the mouth opening, high flow velocities occur early in the strike while the mouth area is still relatively small (equation (2.1); figure 2).

If, instead of a single expanding cone, we model the oral cavity of the fish as three interconnected cones that can expand independently, it is possible to incorporate an anterior-to-posterior wave of expansion into the model. When we allowed the posterior cones to continue to expand after the time of peak gape, we found that the timing of the velocity peak shifted closer to the time of peak gape. Figure 5 shows the effect of different combinations of time delays in the two posterior cone sections on the coordination of peak gape with peak velocity. A distinct ridge appears in the contour plot, indicating optimal combinations. By manipulating this model, we were able to generate flow profiles with a single velocity peak that coincided with peak gape (figure 6), but the conditions that allowed this were highly constrained.

Of the 304 980 simulations that met our criteria for an anterior-to-posterior wave of expansion, only 1123 (0.37%) produced velocity profiles with a single peak that occurred between 90 and 110 per cent of the time of peak gape. Figure 7 illustrates the relatively small volume of space occupied by simulations that resulted in realistic flow profiles relative to the total parameter space tested. The parameters that played the largest role in determining the velocity profile were the length of the anterior cone, the time delay for the onset of section 2 and α.

Anterior cones that were short relative to the total length of the buccal cavity were most likely to produce a realistic velocity profile (figure 7). The longer the anterior cone, the more constrained the rest of the parameters (figure 7). For example, with an anterior cone length of 14 mm, only $\alpha = 8$ and section 2 delay of 12–14% of total strike time produced an appropriate velocity profile. Shorter anterior cones allowed much greater flexibility in the other parameters. For an anterior mouth length of 2 mm, α values between 4 and 9 and section 2 delays between 4 and 17 per cent of strike time produced acceptable velocity profiles. Therefore, the longer the anterior mouth cone, the more precisely the fish has to coordinate the rest of the strike parameters, whereas a shorter anterior cone allows more freedom in the coordination of the other strike parameters.

The velocity profile was also sensitive to the time lag between the mouth opening and the onset of the expansion of the posterior sections. Realistic velocity profiles were found with time lags between 4 and 17 per cent of the total strike time for section 2, and 12 and 26 per cent of the total strike for section 3. Because the posterior-most section represents the limit of the expanding volume, this section did not expand. In the case of the time delay for section 2, more moderate values allowed more flexibility in the other parameters (figure 7). A delay of 12 per cent allowed α values between 4 and 9 and anterior cone lengths between 2 and 14 mm. A delay of 8 per cent, however, required an α value of 7 or 8 and an anterior cone length of 2 mm. Delays of 17 per cent put similar constraints on the other parameters, allowing only α values of 7 or 8 and an anterior cone length of 2 mm.

Relatively high α values were more likely to produce a realistic velocity profile, such that the movement of the mouth began gradually, and then accelerated rapidly (figure 2*b*). Realistic velocity profiles were produced with α values between 4 and 9. A value of 8 gave the greatest flexibility in the other parameters, allowing anterior cone lengths of 2–14 mm and section 2 delays between 4 and 17 per cent of strike time. Lower α values required the anterior cones to be shorter, 2–8 mm, and the onset delay for section 2 to be 8–12% of the strike.

Among the simulations that did not produce a realistic velocity profile, long anterior cones and low α values tended to cause a small peak in velocity early in the strike in addition to the larger peak later in the strike. This secondary early peak has not been observed in empirical measurements (Ferry-Graham *et al.* 2003; Day *et al.* 2005; Higham *et al.* 2006). This peak appears because these conditions promote a large volume increase in the mouth while the mouth area is still relatively small, causing high velocities early in the strike. Delaying the onset of the expansion of the posterior end of cone 1 (which is also the anterior end of cone 2), minimizing the length of cone 1 and having a gradual increase in gape early in the strike all help to limit the volume increase when the gape is very small.

The position of the velocity peak was also sensitive to the relative timing of the onset of the expansion of the mouth sections and to the α value. All else being equal, shorter onset delays for the posterior sections tended to shift the velocity peak earlier in the strike (figure 8*a*), whereas longer onset delays caused it to occur later. Similarly, lower values of α caused the velocity peak to occur earlier in the strike, whereas higher values made it occur later (figure 8*b*). The combination of the relatively large volume expansion posteriorly and the precise pattern of time lags and accelerations allowed the maximum rate of change in mouth volume to coincide with peak gape (figure 6).

The full exploration of these parameters through simulation allows predictions to be made about what combinations of parameters produce the greatest flow velocities (figure 9). The greatest velocities were attained with short anterior cone lengths and high α values (figure 9*a*). Interestingly, the highest peak velocities were also found with high onset delay times for mouth section 2 (figure 9*b*), which place the greatest constraints on the other parameter values (anterior cone length has to be very short and α very high). This suggests that there may be a cost to maximizing fluid speed in that it requires more precise coordination of movements of the mouth. Therefore, it is possible that fishes rarely produce flow velocities as high as the maxima predicted here because the necessary level of coordination cannot be achieved consistently. Because there was an uncertainty regarding the unexpanded

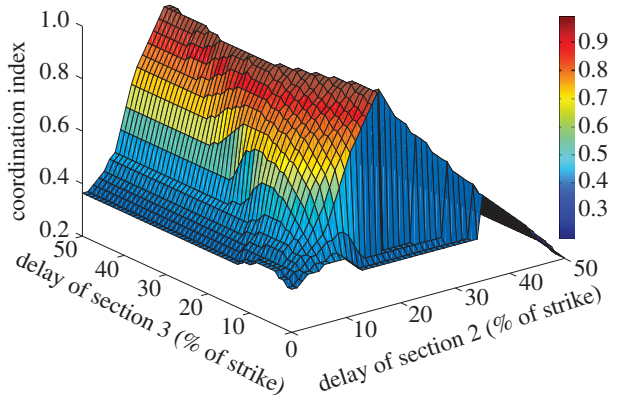

Figure 5. Surface plot of coordination between peak velocity and peak gape as a function of delays in sections 2 and 3 in the three-cone model. The coordination index is equal to $CI = 1 - (|t_{pvel} - t_{pgape}|)/t_{pvel}$ where t_{pvel} is the time to peak velocity and t_{pgape} is the time to peak gape. CI equals 1 if peak velocity and gape are exactly coordinated and is proportionately lower for greater deviations of peak gape from peak velocity. The surface shows the greatest value of CI found for each combination of delays for sections 2 and 3. Because there are other variables that affect CI, there is a cloud of points beneath the surface. This plot represents results from all of the simulations; so any of the points on the surface could represent combinations that were ultimately rejected as unrealistic results because they produced a second velocity peak.

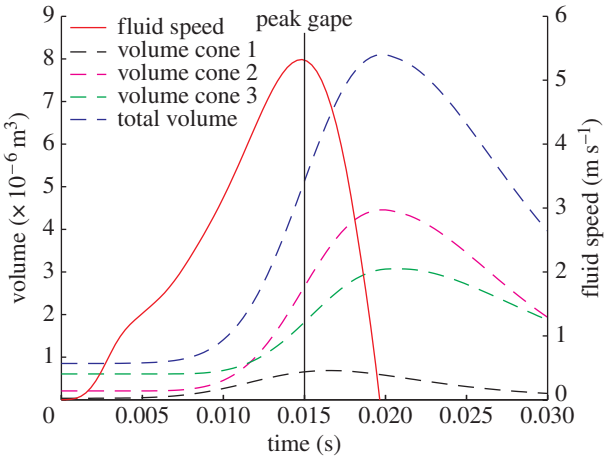

Figure 6. Buccal cavity volume change and fluid velocity at the mouth opening through a sample strike using a three-cone geometry. For this simulation, $\alpha = 7$, anterior cone length was 2 mm, onset delay for section 2 was 15% and onset delay for section 3 was 25% of total strike time. Peak velocity occurs just before peak gape and its magnitude is greatly reduced relative to figures 3 and 4.

mouth dimensions in living fishes, the absolute magnitudes of the velocities are subject to error, but the relative magnitudes of peak velocities are not affected.

4. DISCUSSION

The timing of peak velocity relative to the gape cycle is probably very important to prey capture success. The larger the mouth opening, the greater the likelihood that a prey item will enter. Also, the size of the flow field external to the mouth has been shown to scale directly with the diameter of the mouth opening (Day *et al.* 2005); therefore the flow field is also the largest at peak gape, maximizing the probability of prey capture success at that time. However, in the absence of an anterior-to-posterior wave of oral expansion, peak flow velocity occurs at a time when the mouth area is less than half of its maximum, reducing the probability of prey capture success. Recent evidence suggests that flow acceleration has a larger effect on the forces a prey item encounters than flow velocity (Holzman *et al.* 2007; Wainwright & Day 2007) and the captured prey item typically enters the mouth slightly before the time of peak flow velocity in the bluegill sunfish and largemouth bass (Day *et al.* 2005; Higham *et al.* 2006). Maximum acceleration occurs even earlier in the strike than peak velocity; so without the wave of expansion the greatest forces exerted on the prey item occur when the mouth is much less than half of its maximum gape (figure 4).

By contrast, incorporating a wave of expansion into the model places the maximum flow velocity concurrent with maximum gape and places the maximum fluid acceleration from the time when the gape is a little over half of maximum until it is very near maximum gape

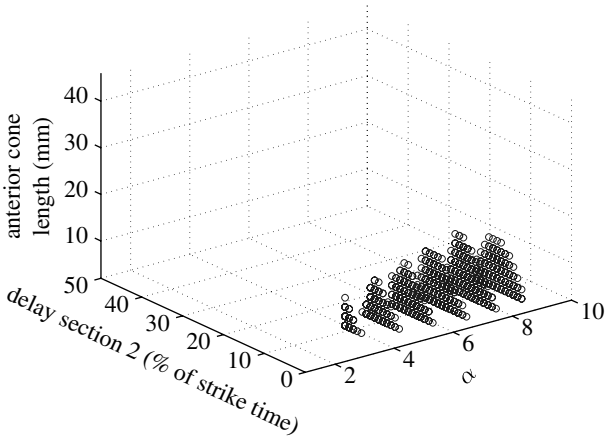

Figure 7. Three-dimensional representation of the total parameter space tested for α, anterior cone length and onset delay for section 2 with solutions plotted that resulted in a single velocity peak occurring between 45 and 55% of the total strike time. The volume of parameter space occupied by solutions that meet these criteria is relatively small, 0.37% of 304 980 possible combinations.

(figure 6). It is interesting to note that despite similar expansion parameters for the single and three-cone models, the maximum velocity for the single cone was greater at all time lags than for the three-cone model. The maximum flow velocities predicted by the three-cone model (figure 9) are somewhat higher than the highest velocities measured for the bluegill sunfish, approximately 3.5 m s^{-1} (Day *et al.* 2005). These predictions would probably be improved by better information about the dimensions of the buccal cavity prior to expansion and about the role of the opercular cavity during expansion. Nevertheless, the peak velocities predicted by the three-cone model represent an improvement to the single-cone model, which predicted unrealistically high maximum flow speeds of up to 30 m s^{-1}. Spreading out the volume expansion over a larger proportion of the strike results in slower flow velocities because the same amount of expansion

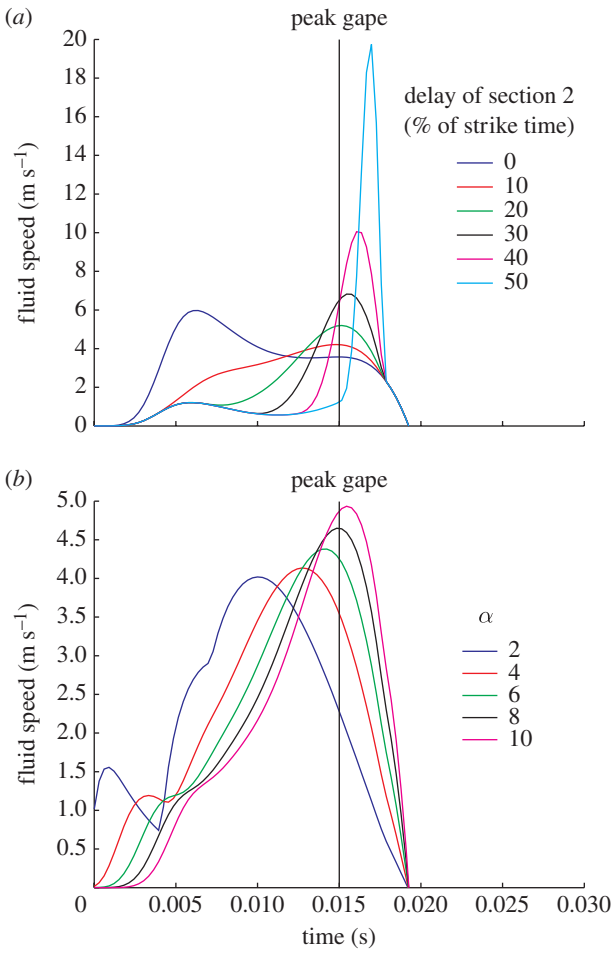

Figure 8. Effect of (*a*) onset delay of the expansion of section 2 and (*b*) α on the timing of peak velocity with all other variables held constant in the three-cone model. For all of these simulations, anterior cone length was set to 4 mm; in (*a*) α was set to 7 and in (*b*) the onset delay for section 2 was set to 12% of strike time. Longer delays and higher α values caused velocity to peak later in the strike. Note that many of these combinations do not meet the criteria for a realistic strike.

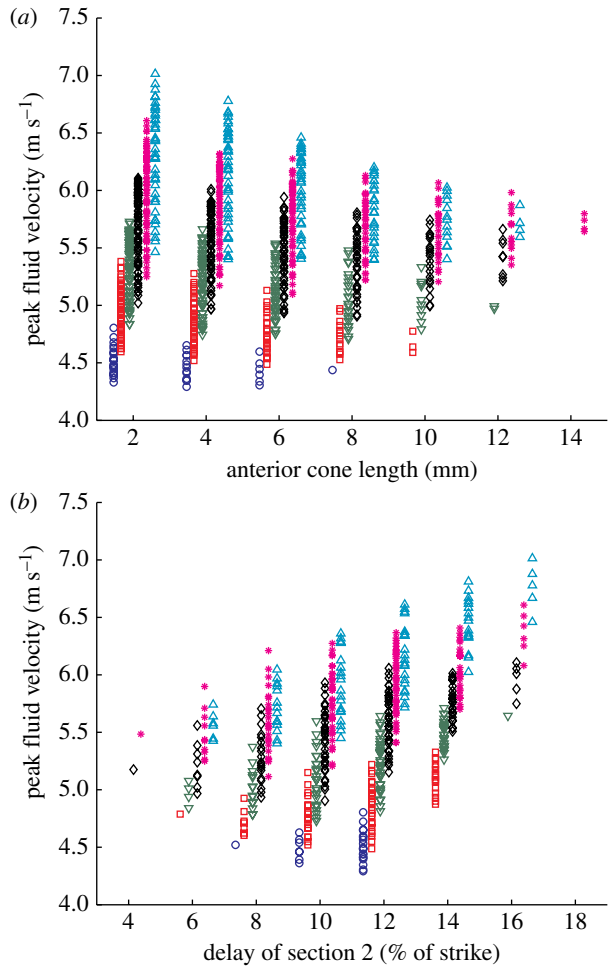

Figure 9. Peak fluid velocity for strikes with a single peak that occurs between 90 and 110% of time to peak gape as a function of (*a*) anterior cone length and α and (*b*) onset delay of the expansion of section 2 and α (circles, 4; squares, 5; down triangles, 6; diamonds, 7; asterisks, 8; up triangles, 9). The highest peak velocities are reached at short anterior cone lengths, high α values and long delays. Note that the points for different α values have been offset for clarity. All vertical clusters of points correspond to the value below the centre of the cluster on the x-axis.

occurs over a longer period of time, resulting in a lower rate of volume change. This suggests a trade-off between maximizing flow velocity and optimizing the timing of peak flow so that it coincides with peak gape.

The highly constrained nature of the parameters that allow flow velocity to be coordinated with mouth kinematics raises interesting questions about the mechanisms by which this coordination is regulated. While the α values that reflect the acceleration patterns of the movement are likely to be under neuromuscular control, it is possible that the timing of the anterior-to-posterior wave of expansion is mechanically determined. Fish skulls are complex with highly kinetic musculoskeletal systems. The jaws and buccal expansion system consist of complex linkage systems that transmit force and motion through multiple interconnected joints. An interesting hypothesis that arises from the results of this study is that the precise timing of movements of different regions of the mouth is built into these mechanical linkages. If so, this would suggest that the mechanical linkages that coordinate movements of the skull during feeding have been tuned by natural selection to the precise timing that optimizes flow velocity relative to gape.

Although the timing of peak flow velocity relative to the gape cycle is likely to be extremely important to prey capture success, the range of parameters which allows this coordination appears to be very tightly constrained. First, the volume change in the middle chamber must be large relative to the volume change in the anterior chamber. The generation of suction is thought to be largely driven by depression of the hyoid (Lauder 1985; De Visser & Barel 1996; Sanford & Wainwright 2002), and the results found here are consistent with that view, as the position of the hyoid is represented here by the middle cone. Second, the initial rate of expansion of the anterior chamber must be slow to prevent large flow velocities when the area of the mouth opening is small. Third, the anterior-to-posterior wave of expansion allows the rate of volume increase in the buccal cavity, and therefore the fluid velocity at the mouth, to be high at the time of peak gape because the posterior chambers are still expanding at that time.

Without an anterior-to-posterior wave of expansion, the entire mouth volume increases simultaneously, which results in a greater rate of volume expansion, and therefore greater maximum flow velocity than if the expansion continues after peak gape. It appears therefore that coordination of flow velocity with gape kinematics is more important to prey capture success than simply maximizing flow velocity.

We would like to thank Rita Mehta for helpful discussions and comments on this manuscript and Adam Summers for assistance with figure 1. This manuscript was greatly improved by the comments of four anonymous reviewers. This work was supported by NSF awards DBI-0630670 and IOB-0444554.

REFERENCES

Carroll, A. M. & Wainwright, P. C. 2003 Functional morphology of prey capture in the sturgeon, *Scaphirhynchus albus*. *J. Morphol.* **256**, 270–284. (doi:10.1002/jmor.10095)

Day, S. W., Higham, T. E., Cheer, A. Y. & Wainwright, P. C. 2005 Spatial and temporal patterns of water flow generated by suction-feeding bluegill sunfish *Lepomis macrochirus* resolved by particle image velocimetry. *J. Exp. Biol.* **208**, 2661–2671. (doi:10.1242/jeb.01708)

De Visser, J. & Barel, C. D. N. 1996 Architectonic constraints on the hyoid's optimal starting position for suction feeding of fish. *J. Morphol.* **228**, 1–18. (doi:10.1002/(SICI)1097-4687(199604)228:1<1::AID-JMOR1>3.0.CO;2-B)

Drost, M. R. & van den Boogaart, J. G. M. 1986 A simple method for measuring the changing volume of small biological objects, illustrated by studies of suction feeding by fish larvae and of shrinkage due to histological fixation. *J. Zool. Lond. (A)* **209**, 239–249.

Drost, M. R., Muller, M. & Osse, J. W. M. 1988 A quantitative hydrodynamical model of suction feeding in larval fishes: the role of frictional forces. *Proc. R. Soc. B* **234**, 263–281. (doi:10.1098/rspb.1988.0048)

Ferry-Graham, L. A. 1997 Feeding kinematics of juvenile swellsharks, *Cephaloscyllium ventriosum*. *J. Exp. Biol.* **200**, 1255–1269.

Ferry-Graham, L. A. & Lauder, G. V. 2001 Aquatic prey capture in ray-finned fishes: a century of progress and new directions. *J. Morphol.* **248**, 99–119. (doi:10.1002/jmor.1023)

Ferry-Graham, L. A., Wainwright, P. C. & Lauder, G. V. 2003 Quantification of flow during suction feeding in bluegill sunfish. *Zoology* **106**, 159–168. (doi:10.1078/0944-2006-00110)

Gibb, A. C. & Ferry-Graham, L. 2005 Cranial movements during suction feeding in teleost fishes: are they modified to enhance suction production? *Zoology* **108**, 141–153. (doi:10.1016/j.zool.2005.03.004)

Higham, T. E., Day, S. W. & Wainwright, P. C. 2006 The pressures of suction feeding: the relation between buccal pressure and induced fluid speed in centrarchid fishes. *J. Exp. Biol.* **209**, 3281–3287. (doi:10.1242/jeb.02383)

Holzman, R., Day, S. W. & Wainwright, P. C. 2007 Timing is everything: coordination of strike kinematic affects the force exerted by suction feeding fish on attached prey. *J. Exp. Biol.* **210**, 3328–3336. (doi:10.1242/jeb.008292)

Lauder, G. V. 1980*a* Evolution of the feeding mechanism in primitive actinopterygian fishes: a functional anatomical analysis of *Polypterus*, *Lepisosteus*, and *Amia*. *J. Morphol.* **163**, 283–317. (doi:10.1002/jmor.1051630305)

Lauder, G. V. 1980*b* The suction feeding mechanism in sunfishes (*Lepomis*): an experimental analysis. *J. Exp. Biol.* **88**, 49–72.

Lauder, G. V. 1983 Prey capture hydrodynamics in fishes—experimental tests of two models. *J. Exp. Biol.* **104**, 1–13.

Lauder, G. V. 1985 Aquatic feeding in lower vertebrates. In *Functional vertebrate morphology* (eds M. Hildebrand, D. M. Bramble, K. F. Liem & D. B. Wake), pp. 210–229. Cambridge, MA: Harvard University Press.

Lauder, G. V. & Shaffer, H. B. 1985 Functional morphology of the feeding mechanism in aquatic Ambystomatid salamanders. *J. Morphol.* **185**, 297–326. (doi:10.1002/jmor.1051850304)

Motta, P. J., Hueter, R. E., Tricas, T. C. & Summers, A. P. 2002 Kinematic analysis of suction feeding in the nurse shark, *Ginglymostoma cirratum* (Orectolobiformes, Ginglymostomatidae). *Copeia* **2002**, 24–38. (doi:10.1643/0045-8511(2002)002[0024:KAOSFI]2.0.CO;2)

Muller, M., Osse, J. W. M. & Verhagen, J. H. G. 1982 A quantitative hydrodynamical model of suction feeding in fish. *J. Theor. Biol.* **95**, 49–79. (doi:10.1016/0022-5193(82)90287-9)

Reilly, S. M. 1995 The ontogeny of aquatic feeding behavior in *Salamandra salamandra*: stereotypy and isometry in feeding kinematics. *J. Exp. Biol.* **198**, 701–708.

Sanford, C. P. J. & Wainwright, P. C. 2002 Use of sonomicrometry demonstrates the link between prey capture kinematics and suction pressure in largemouth bass. *J. Exp. Biol.* **205**, 3445–3457.

Summers, A. P., Darouian, K. F., Richmond, A. M. & Brainerd, E. L. 1998 Kinematics of aquatic and terrestrial prey capture in *Terrapene carolina*, with implications for the evolution of feeding in Cryptodire turtles. *J. Exp. Zool.* **281**, 280–287. (doi:10.1002/(SICI)1097-010X(19980701)281:4<280::AID-JEZ4>3.0.CO;2-K)

van Leeuwen, J. L. & Muller, M. 1983 The recording and interpretation of pressures in prey-sucking fish. *Neth. J. Zool.* **33**, 425–475. (doi:10.1163/002829683x00192)

van Leeuwen, J. L. & Muller, M. 1984 Optimum sucking techniques for predatory fish. *Trans. Zool. Soc. Lond.* **37**, 137–169.

Van Wassenbergh, S., Herrel, A., Adriaens, D. & Aerts, P. 2004 Effects of jaw adductor hypertrophy on buccal expansions during feeding of air breathing catfishes (Teleostei, Clariidae). *Zoomorphology* **123**, 81–93. (doi:10.1007/s00435-003-0090-3)

Van Wassenbergh, S., Aerts, P. & Herrel, A. 2006*a* Hydrodynamic modelling of aquatic suction performance and intra-oral pressures: limitations for comparative studies. *J. R. Soc. Interface* **3**, 507–514. (doi:10.1098/rsif.2005.0110)

Van Wassenbergh, S., Aerts, P. & Herrel, A. 2006*b* Scaling of suction feeding performance in the catfish *Clarias gariepinus*. *Physiol. Biochem. Zool.* **79**, 43–56. (doi:10.1086/498188)

Wainwright, P. C. & Day, S. W. 2007 The forces exerted by aquatic suction feeders on their prey. *J. R. Soc. Interface* **4**, 553–560. (doi:10.1098/rsif.2006.0197)

Wilga, C. D. & Motta, P. J. 1998*a* Conservation and variation in the feeding mechanism of the spiny dogfish *Squalus acanthias*. *J. Exp. Biol.* **201**, 1345–1358.

Wilga, C. D. & Motta, P. J. 1998*b* Feeding mechanism of the Atlantic guitarfish *Rhinobatos lentiginosus*: modulation of kinematic and motor activity. *J. Exp. Biol.* **201**, 3167–3184.